



Published in final edited form as:

Nature. 2016 November 24; 539(7630): 546–550. doi:10.1038/nature19849.

Catalytic activation of carbon–carbon bonds in cyclopentanones

Ying Xia^{1,2}, Gang Lu³, Peng Liu³, and Guangbin Dong^{1,2}

¹Department of Chemistry, University of Texas at Austin, Austin, Texas 78712, USA

²Department of Chemistry, University of Chicago, Chicago, Illinois 60637, USA

³Department of Chemistry, University of Pittsburgh, Pittsburgh, Pennsylvania 15260, USA

Abstract

In the chemical industry, molecules of interest are based primarily on carbon skeletons. When synthesizing such molecules, the activation of carbon–carbon single bonds (C–C bonds) in simple substrates is strategically important: it offers a way of disconnecting such inert bonds, forming more active linkages (for example, between carbon and a transition metal) and eventually producing more versatile scaffolds^{1–13}. The challenge in achieving such activation is the kinetic inertness of C–C bonds and the relative weakness of newly formed carbon–metal bonds^{6,14}. The most common tactic starts with a three- or four-membered carbon-ring system^{9–13}, in which strain release provides a crucial thermodynamic driving force. However, broadly useful methods that are based on catalytic activation of unstrained C–C bonds have proven elusive, because the cleavage process is much less energetically favourable. Here we report a general approach to the catalytic activation of C–C bonds in simple cyclopentanones and some cyclohexanones. The key to our success is the combination of a rhodium pre-catalyst, an *N*-heterocyclic carbene ligand and an amino-pyridine co-catalyst. When an aryl group is present in the C3 position of cyclopentanone, the less strained C–C bond can be activated; this is followed by activation of a carbon–hydrogen bond in the aryl group, leading to efficient synthesis of functionalized α -tetralones—a common structural motif and versatile building block in organic synthesis. Furthermore, this method can substantially enhance the efficiency of the enantioselective synthesis of some natural products of terpenoids. Density functional theory calculations reveal a mechanism involving an intriguing rhodium-bridged bicyclic intermediate.

The most common strategy for cleaving a C–C bond uses a ring system, in which the unfavourable energetics of C–C cleavage can be compensated for by the release of strain in the ring. However, although there has been success in activating C–C bonds in cyclopropane

Reprints and permissions information is available at www.nature.com/reprints.

Correspondence and requests for materials should be addressed to P.L. (pengliu@pitt.edu) and G.D. (gbdong@uchicago.edu).

Supplementary Information is available in the online version of the paper.

Author Contributions Y.X. and G.D. conceived and designed the experiments. Y.X. performed the experiments. G.L. performed the DFT calculations. Y.X., G.L., P.L. and G.D. co-wrote the manuscript.

The authors declare no competing financial interests.

Readers are welcome to comment on the online version of the paper.

Reviewer Information *Nature* thanks J. Harvey, M. Lautens and the other anonymous reviewer(s) for their contribution to the peer review of this work.

and cyclobutane derivatives (Fig. 1a)^{9–13}, the catalytic C–C activation of less strained or non-strained rings is underdeveloped. The rhodium-mediated decarbonylation of cycloalkanones has been described³; unfortunately, however, C–C activation for the less strained cyclopentanone showed low efficiency (Fig. 1b). For larger cyclic structures, an innovative chelation-based strategy has also been developed, in which ketimines prepared from the corresponding ketones and 2-amino-3-picoline allowed a directed C–C activation through a five-membered metallacycle^{8,15}. However, although medium to large cyclic ketimines can be efficiently activated in this way, the strategy is problematic for cyclopentanone- and cyclohexanone-derived ketimines (Fig. 1c)¹⁵. Our laboratory recently developed a catalytic C–C activation of isatins, a less strained ring system, to afford 2-quinolinones via decarbonylation and alkyne insertion¹⁶; however, a pre-installed pyridine directing group proved essential. Hence, to our knowledge, catalytic C–C activation of normal cyclopentanones remains an unmet challenge^{17,18}.

It has been postulated that the major difficulty comes from the reversibility of the C–C activation step (Fig. 1d)^{1,6,19}. In contrast to three- or four-membered rings, cyclopentanones lack sufficient thermodynamic driving forces to favour oxidative addition with a transition metal⁶; instead, the reverse process—C–C reductive elimination—is often preferred (Fig. 1d)^{1,19}. We hypothesized that such a problem could be solved by merging an unfavourable C–C activation with a tandem *sp*² C–H functionalization to enable an overall thermodynamically favoured transformation¹³. As depicted in Fig. 1e, installing an aryl group at cyclopentanone's C3 position should allow the transient C–C activation intermediate (**B**) generated using Jun's temporary directing strategy⁸ to undergo an intramolecular ortho C–H activation, to give rhodacycle (**C**). Subsequent *sp*²–*sp*² reductive elimination would ultimately lead to α -tetralone derivatives—well known building blocks used by the chemical industry and common structural motifs found in bioactive compounds^{20–23}. The whole catalytic process would convert an aliphatic ketone to a more stable aryl ketone, accounting for the overall thermodynamic benefits of this transformation (ΔG would be about -6 kcal mol^{-1}).

To test our hypothesis, we chose 3-phenylcyclopentanone (**1a** in Fig. 2) as the model substrate. After a survey of various reaction parameters (see Supplementary Information and Supplementary Figs 1, 2), we found that using $[\text{Rh}(\text{C}_2\text{H}_4)_2\text{Cl}]_2$ as the catalyst precursor and 2-aminopyridine (**C1**) as the co-catalyst in 1,4-dioxane indeed offered the desired C–C activation products, with an 85% yield (Supplementary Table 1, entry 1). We observed two skeleton-rearranged products, in a 6.4:1 ratio. The major product, α -tetralone (**1b**), came from the cleavage of the more hindered C1–C2 bond; the minor product, α -indanone (**1c**), was generated from the cleavage of the less hindered C1–C5 bond. Further study revealed that $[\text{Rh}(\text{C}_2\text{H}_4)_2\text{Cl}]_2$ is a superior pre-catalyst, while others are much less efficient (Supplementary Table 1, entries 2–4). We investigated a series of 2-aminopyridines, and the simple 2-aminopyridine (**C1**) remained optimal; in contrast, the secondary amines (**C2** and **C3**) exhibited almost no reactivity (Supplementary Table 1, entries 5–7). In terms of ligands, the unsaturated *N*-heterocyclic carbenes IMes (1,3-bis(2,4,6-trimethylphenyl)imidazol-2-ylidene) and the bulkier IPr (1,3-bis(2,6-diisopropylphenyl)imidazol-2-ylidene) afforded comparable results (Supplementary Table 1, entry 8); in contrast, saturated *N*-heterocyclic

carbenes (such as SIMes: 1,3-bis(2,4,6-trimethylphenyl)-4,5-dihydroimidazol-2-ylidene) showed substantially diminished reactivity (Supplementary Table 1, entry 9). Note that phosphine ligands, such as PCy₃ and BINAP (2,2'-bis(diphenylphosphino)-1,1'-binaphthyl), failed to promote the transformation (Supplementary Table 1, entries 10, 11). Interestingly, lowering the loading of amine co-catalyst **C1** enhanced the regioselectivity, such that the α -tetralone product was formed almost exclusively, albeit with a compromised yield (Supplementary Table 1, entry 12). Increasing the reaction temperature failed to improve the yield (Supplementary Table 1, entry 13), but addition of 50 mol% of water increased the yield to 86% without loss of regioselectivity (Supplementary Table 1, entry 14).

We then investigated the substrate scope of this C–C activation reaction (Fig. 2). Under optimized reaction conditions (condition A: 25 mol% of the co-catalyst 2-aminopyridine; temperature 140 °C), standard substrate **1a** gave a somewhat lower yield when the reaction was run on a 0.2 mmol or 1.0 mmol scale. Under a slightly modified condition (condition B: 50 mol% of 2-aminopyridine; temperature 150 °C), the conversion of **1a** increased and the major product (**1b**) was isolated at a yield of 73%, although the regioselective ratio (r.r.) dropped from >10:1 to 5.8:1. Substrates bearing an electron-neutral or electron-rich substituent at the para-position of the aryl ring afforded comparable yields (products **2b–6b**). For cyclopentanones with an electron-deficient aryl group, the reactions were much slower under condition A; however, a decent yield and excellent regioselectivity could be achieved under condition B (products **7b–14b**). A wide range of functional groups—such as ester, ketone, fluoride, aryl chloride, cyano, sulfonyl, aryl boronate, olefin and free hydroxyl groups—are well tolerated in the products (**7b–16b, 20b**). Meta-substituted arenes are also competent substrates, in which C–H activation occurred site selectively at the less hindered position (products **17b, 18b**). The more sterically encumbered (ortho-substituted) substrates **19a** and **20a** still exhibited high reactivity. In particular, naphthyl-substituted cyclopentanones were smoothly converted to tricyclic compounds (**21b, 22b**); a quaternary centre at the C3 position did not affect the efficiency of this reaction, although the regioselectivity decreased to some extent (products **23b, 24b**). As expected, the reaction was sluggish for cyclopentanones bearing a C2 substituent (for example, **25a**); nevertheless, C–C activation still occurred predominantly at the more hindered site (to produce **25b**). Moreover, the 3,4-disubstituted and ring-fused cyclopentanones are also suitable substrates, and the relative configuration is preserved during the reaction (products **26b, 27b**). Finally, this method allows the preparation of unusual derivatives of complex bioactive molecules (**28b** and **29b**). For example, a fused ring can be conveniently installed on oestrone (to produce **29b**).

Compared with cyclopentanones, cyclohexanones are generally less strained (see the computed ring strains in Supplementary Information), and thus are more challenging substrates for C–C activation¹⁵. Indeed, under our standard conditions (A or B), no C–C activation or rearrangement product was observed when using 3-arylcyclohexanones (for example, **30a** or **35a**) as the substrate. However, when using the bulkier IPr as the ligand and 2-amino-6-picoline as the co-catalyst (Fig. 2b, condition C), the C–C activation product **30c** was isolated in 34%–46% yield (67%–73% yield on the basis of recovered starting material).

For example, the C1–C6 bond of cyclohexanone **30a** was exclusively cleaved to furnish the product α -indanone, giving the opposite regioselectivity from cyclopentanones. In addition, cyclohexanone substrates containing electron-rich or electron-deficient aryl groups show comparable reactivity (products **31c–33c**). Moreover, heterocyclic substrates, such as **34a**, also underwent the C–C activation/rearrangement to produce alkoxy-substituted α -indanone (**34c**). The quaternary centre in the cyclohexanones appears to facilitate the C–C/C–H activation process, as 3-phenylcyclohexanone (**35a**) only afforded a trace amount of the product (**35c**). The 6,6-fused cyclohexanone **36a** can also undergo this transformation to afford a spirocyclic α -indanone (**36c**).

To demonstrate the practicability of this transformation, we carried out gram-scale reactions (Fig. 3a), which offered either a higher yield compared with the small-scale reaction (when using substrate **9a**; see above and Fig. 2) or a lower catalyst loading (when using substrate **24a**). To show the versatile nature of α -tetralones in organic synthesis, we introduced several new functional moieties to C–C activation product **9b** through standard protocols (Fig. 3b). The synthetic potential of this method can be further demonstrated in the asymmetric syntheses of natural products (Fig. 3c). For example, α -tetralone (**2b**) is a known intermediate for accessing erogorgiaene^{20,21}, (*R*)-ar-himachalene²² and (–)-heliophenanthrone²³ in three to seven steps; however, enantioselective preparation of α -tetralones with a C4 stereocentre is non-trivial and generally requires many steps²². Given that optically enriched 3-arylcyclopentanones can be synthesized in a single step from asymmetric conjugate addition between cyclopentenone and arylboronic acids²⁴, using the C–C activation approach we isolated α -tetralone ((*R*)-**2b**) in 64% yield over two steps, with 94.5% chirality transfer. The slight decrease in enantioselectivity was probably caused by a reversible β -H elimination process with the C–C activation intermediate (see rhodacycle **B** above; Fig. 1e). With an efficient route to (*R*)-**2b**, the synthesis of the aforementioned terpenoids is markedly streamlined.

To better understand the origin of the regioselectivity and the mechanism of the C–H metallation step, we carried out density functional theory (DFT) calculations. The computed free energy profile of the key steps in the catalytic cycle is shown in Fig. 4a. Through the installation of a temporary directing group, the resulting ketimines (both *E* and *Z* isomers) can initially bind to the rhodium in a bidentate fashion to form **41a** and **41b**. The pyridyl group remains bound to the metal and promotes C–C oxidative addition (via transition states **TS1** and **TS2**, Fig. 4b). While cleavage of the sterically more hindered C1–C2 bond in **TS1** is slightly less favoured, activations of the C1–C2 and C1–C5 bonds are both reversible, with a relatively low activation barrier. Indeed, the regioselectivity is determined in the subsequent C–H metallation step (via **TS3** and **TS4**) and C–C reductive elimination step (via **TS5** and **TS6**)—both steps requiring much higher activation energies than that of the C–C cleavage. The pathway with rhodacycle **42a** (derived from activation of the C1–C2 bond) has lower barriers in both C–H metallation (**TS3**) and C–C reductive elimination (**TS5**) than the corresponding reaction with rhodacycle **42b** (derived from activation of the C1–C5 bond).

The substantial destabilization of the disfavoured transition states (**TS4** and **TS6**) is caused mainly by the steric repulsions between the C5 methylene group in the forming six-

membered rhodacycle and the ortho methyl group on the IMes ligand. This unfavourable interaction in **TS4** is evidenced by the short hydrogen–hydrogen distance of 2.08 Å (Fig. 4c). In contrast, these steric repulsions are diminished in **TS3** and **TS5**, in which the methylene group is positioned further away from the IMes ligand owing to the shorter tether in the forming five-membered metallacycle. The strong kinetic preference for the pathway involving the 5,6-bridged rhodacycle **43a** explains the high level of regioselectivity for the C1–C2-activation product. The subsequent protonation (Supplementary Fig. 12) requires lower barriers and provides thermodynamic driving forces to finally form α -tetralone (**1b**) upon hydrolysis. Regarding the C–H metallation step, we found that a chloride-mediated metallation-deprotonation pathway²⁵ was more favourable; in contrast, concerted 1,4-rhodium migration^{26–30} through σ -bond metathesis can be ruled out owing to the much higher activation energy required.

This computationally proposed mechanism is also consistent with observed kinetic isotope effects and with isotope labelling experiments (see Supplementary Information). First, the small primary kinetic isotope effect suggests that the C–H metallation and C–C reductive elimination are both turnover limiting. Second, the incomplete deuterium transfer seen in a reaction with deuterated substrate provides further evidence against the concerted 1,4-rhodium migration mechanism.

Supplementary Material

Refer to Web version on PubMed Central for supplementary material.

Acknowledgments

This project was supported by the Cancer Prevention Research Institute of Texas (grant R1118), the National Institute of General Medical Science (grant R01GM109054) and the Welch Foundation (grant F1781). G.D. is a Searle Scholar and Sloan fellow. Y.X. acknowledges the International Postdoctoral Exchange Fellowship Program 2015 from the Office of China Postdoctoral Council (OCPC, document 38, 2015). We thank Johnson Matthey for a donation of Rh salts, and Chiral Technologies for donation of chiral high-performance liquid-chromatography columns. We are grateful to Y. Xu for providing 1,4-dioxane, F. Mo for providing some 3-aryl cyclopentanones, and H. Lim for checking the experimental procedures. DFT calculations were performed using supercomputer resources at the Center for Simulation and Modeling at the University of Pittsburgh, and the Extreme Science and Engineering Discovery Environment supported by the National Science Foundation.

References

1. Gozin M, Weisman A, Ben-David Y, Milstein D. Activation of a carbon–carbon bond in solution by transition-metal-insertion. *Nature*. 1993; 364:699–701.
2. Jones WD. The fall of the C–C bond. *Nature*. 1993; 364:676–677.
3. Murakami M, Amii H, Ito Y. Selective activation of carbon–carbon bonds next to a carbonyl group. *Nature*. 1994; 370:540–541.
4. Rybtchinski B, Milstein D. Metal insertion into C–C bonds in solution. *Angew Chem Int Ed*. 1999; 38:870–883.
5. Murakami M, Ito Y. Cleavage of carbon–carbon single bonds by transition metals. *Top Organomet Chem*. 1999; 3:97–129.
6. Jun CH. Transition metal-catalyzed carbon–carbon bond activation. *Chem Soc Rev*. 2004; 33:610–618. [PubMed: 15592626]
7. Miura M, Satoh T. Catalytic processes involving β -carbon elimination. *Top Organomet Chem*. 2005; 14:1–20.

8. Park YJ, Park JW, Jun CH. Metal–organic cooperative catalysis in C–H and C–C bond activation and its concurrent recovery. *Acc Chem Res.* 2008; 41:222–234. [PubMed: 18247521]
9. Dong, G., editor. C–C bond activation Vol. 346 of *Topics in Current Chemistry*. Springer; 2014.
10. Souillart L, Cramer N. Catalytic C–C bond activations via oxidative addition to transition metals. *Chem Rev.* 2015; 115:9410–9464. [PubMed: 26044343]
11. Seiser T, Saget T, Tran DN, Cramer N. Cyclobutanes in catalysis. *Angew Chem Int Ed.* 2011; 50:7740–7752.
12. Mack DJ, Njardarson JT. Recent advances in the metal-catalyzed ring expansions of three- and four-membered rings. *ACS Catal.* 2013; 3:272–286.
13. Masarwa A, et al. Merging allylic carbon–hydrogen and selective carbon–carbon bond activation. *Nature.* 2014; 505:199–203. [PubMed: 24317692]
14. Halpern J. Determination and significance of transition-metal-alkyl bond dissociation energies. *Acc Chem Res.* 1982; 15:238–244.
15. Jun CH, Lee H, Lim SG. The C–C bond activation and skeletal rearrangement of cycloalkanone imine by Rh(I) catalysts. *J Am Chem Soc.* 2001; 123:751–752. [PubMed: 11456596]
16. Zeng R, Dong G. Rh-catalyzed decarbonylative coupling with alkynes via C–C activation of isatins. *J Am Chem Soc.* 2015; 137:1408–1411. [PubMed: 25569352]
17. Mukai C, Ohta Y, Oura Y, Kawaguchi Y, Inagaki F. Csp³–Csp³ and Csp³–H bond activation of 1,1-disubstituted cyclopentane. *J Am Chem Soc.* 2012; 134:19580–19583. [PubMed: 23146104]
18. Li G, Arisawa M, Yamaguchi M. Rhodium-catalyzed synthesis of unsymmetrical di(aryl/heteroaryl)methanes using aryl/heteroarylmethyl ketones via CO–C bond cleavage. *Chem Commun.* 2014; 50:4328–4330.
19. Albrecht M, Gossage RA, Spek AL, van Koten G. Metal-mediated C–C bond making and breaking: first direct evidence for a reversible migration of a benzyl group along a metal-carbon bond. *J Am Chem Soc.* 1999; 121:11898–11899.
20. Davies HML, Walji AM. Direct synthesis of (+)-erogorgiaene through a kinetic enantiodifferentiating step. *Angew Chem Int Ed.* 2005; 44:1733–1735.
21. Elford TG, Nave S, Sonawane RP, Aggarwal VK. Total synthesis of (+)-erogorgiaene using lithiationborylation methodology, and stereoselective synthesis of each of its diastereoisomers. *J Am Chem Soc.* 2011; 133:16798–16801. [PubMed: 21936552]
22. Chavan SP, Khatod HS. Enantioselective synthesis of the essential oil and pheromonal component ar-himachalene by a chiral pool and chirality induction approach. *Tetrahedron Asymmetry.* 2012; 23:1410–1415.
23. Mukherjee P, Sarkar TK. Heteroatom-directed Wacker oxidations. A protection-free synthesis of (–)-heliophenanthrone. *Org Biomol Chem.* 2012; 10:3060–3065. [PubMed: 22398562]
24. Hayashi T, Yamasaki K. Rhodium-catalyzed asymmetric 1,4-addition and its related asymmetric reactions. *Chem Rev.* 2003; 103:2829–2844. [PubMed: 12914482]
25. Lapointe D, Fagnou K. Overview of the mechanistic work on the concerted metallation deprotonation pathway. *Chem Lett.* 2010; 39:1118–1126.
26. Matsuda T, Shigeno M, Murakami M. Asymmetric synthesis of 3,4-dihydrocoumarins by rhodium-catalyzed reaction of 3-(2-hydroxyphenyl) cyclobutenones. *J Am Chem Soc.* 2007; 129:12086–12087. [PubMed: 17877354]
27. Seiser T, Roth OA, Cramer N. Enantioselective synthesis of indanols from *tert*-cyclobutanols using a rhodium-catalyzed C–C/C–H activation sequence. *Angew Chem Int Ed.* 2009; 48:6320–6323.
28. Shigeno M, Yamamoto T, Murakami M. Stereoselective restructuring of 3-arylcyclobutanols into 1-indanols by sequential breaking and formation of carbon–carbon bonds. *Chem Eur J.* 2009; 15:12929–12931. [PubMed: 19885898]
29. Matsuda T, Suda Y, Takahashi A. Double 1,4-rhodium migration cascade in rhodium-catalysed arylative ring-opening/spirocyclisation of (3-arylcyclobutylidene)acetates. *Chem Commun.* 2012; 48:2988–2990.
30. Matsuda T, Yuihara I. A rhodium(I)-catalysed formal intramolecular C–C/C–H bond metathesis. *Chem Commun.* 2015; 51:7393–7396.

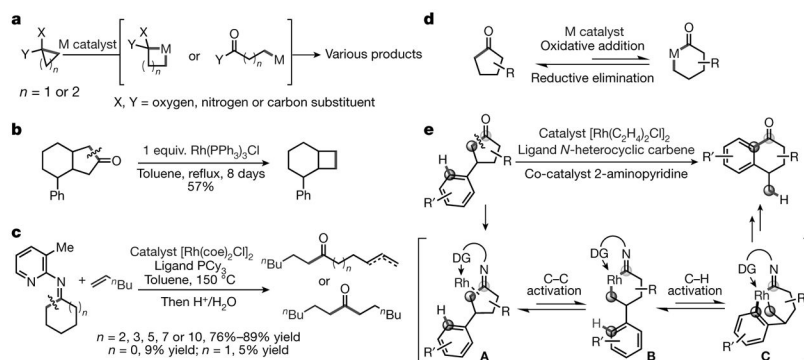
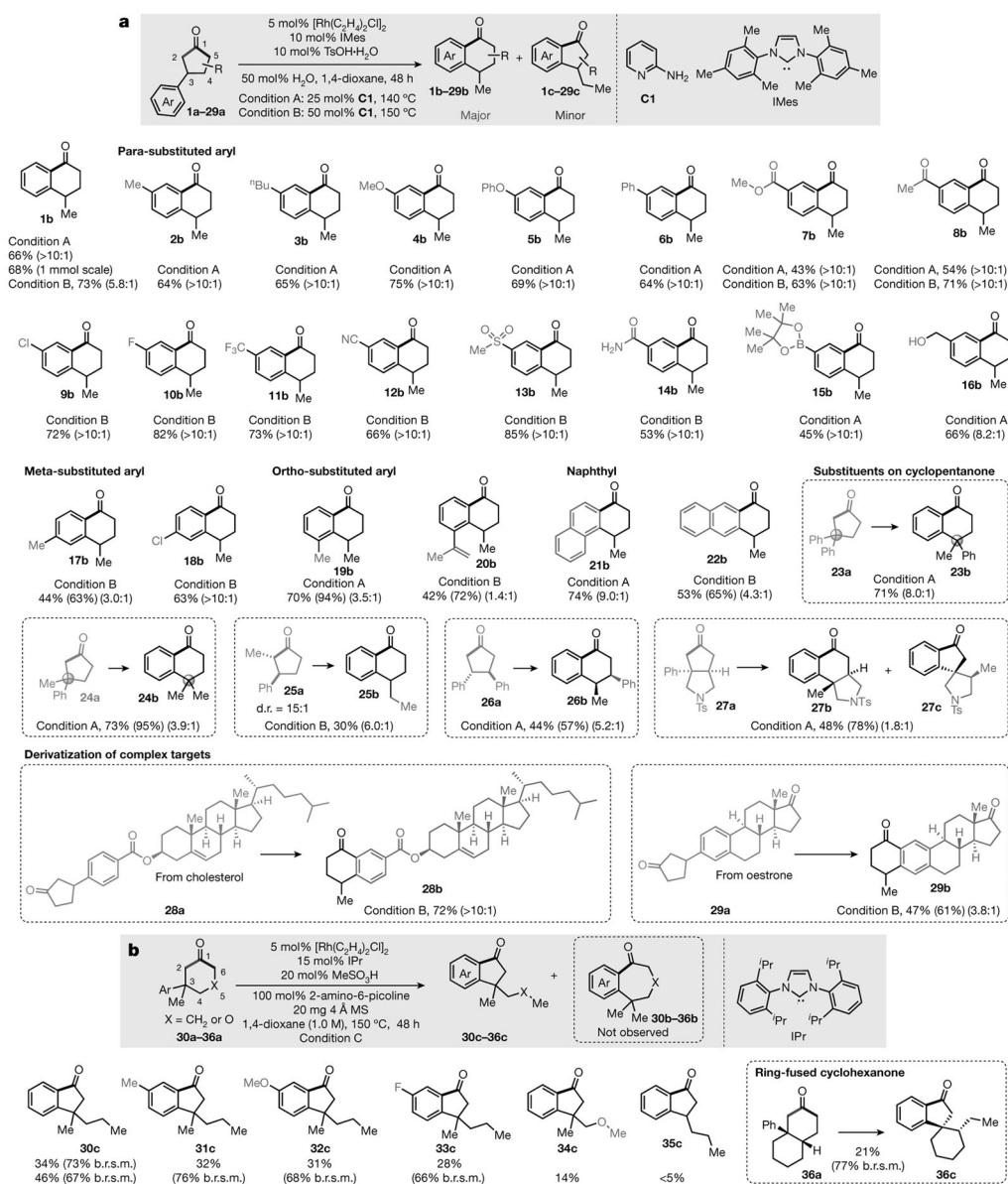


Figure 1. Activation of C–C bonds in ring systems

a. Catalytic C–C activation of strained rings (for example, in cyclopropane or cyclobutanone). The unfavourable energetics of C–C activation can be compensated by the release of strain in the ring. M, transition metal. **b.** Stoichiometric rhodium-mediated C–C activation of less strained cycloketones. This reaction is less efficient than that shown in **a.** Ph, phenyl. **c.** Directed catalytic C–C activation of less strained cycloketimines. The yield is high for large cycloketimines, but low for smaller ones. Bu, butyl; coe, cyclooctene; Me, methyl; PCy₃, tricyclohexylphosphine. **d.** The challenge in terms of activating the C–C bonds of cyclopentanones is that C–C activation is reversible; the thermodynamic driving forces do not always allow oxidative addition with a transition metal, instead favouring the reverse process (C–C reductive elimination). R, hydrocarbon side chain. **e.** Our strategy for catalytic C–C activation of cyclopentanones: merging the unfavourable C–C activation with C–H activation, to produce an overall thermodynamically favoured reaction. Specifically, when using a cyclopentanone with an aryl group in the C3 position, the imine intermediate (**A**; with a pendant directing group, DG) should allow the transient C–C activation intermediate (**B**) to undergo an intramolecular C–H activation, producing rhodacycle (**C**). Subsequent reductive elimination will lead to α -tetralone derivatives.

**Figure 2. Substrate scope**

a, Scope of the cyclopentanones. The shaded box at the top shows the basic reaction: the substrates are 3-arylcyclopentanones (**1a–29a**); the major products, α -tetralones (**1b–29b**), come from cleavage of the more hindered C1–C2 bond, while the minor products, α -indanones (**1c–29c**), are generated through cleavage of the less hindered C1–C5 bond. $[\text{Rh}(\text{C}_2\text{H}_4)_2\text{Cl}]_2$ is the catalyst precursor and 2-aminopyridine (**C1**) is the co-catalyst; TsOH is toluene sulfonic acid. Ar, aryl group. Below the shaded box are shown the major products and their isolated yields. **b**, Scope of the cyclohexanones. See Supplementary Information for further experimental details. The regioselective ratios (r.r.) were determined by gas chromatography-mass spectrometry or ^1H nuclear magnetic resonance (NMR) of the crude products. The percentages in parentheses are the total yields or the b.r.s.m. (based on recovered starting material) yields determined by ^1H NMR, using 1,1,2,2-tetrachloroethane

(TCE) as the internal standard. d.r., diastereomeric ratio; IMes, 1,3-bis(2,4,6-trimethylphenyl)imidazol-2-ylidene; IPr, 1,3-bis(2,6-diisopropylphenyl)imidazol-2-ylidene; MS, molecular sieve.

Author Manuscript

Author Manuscript

Author Manuscript

Author Manuscript

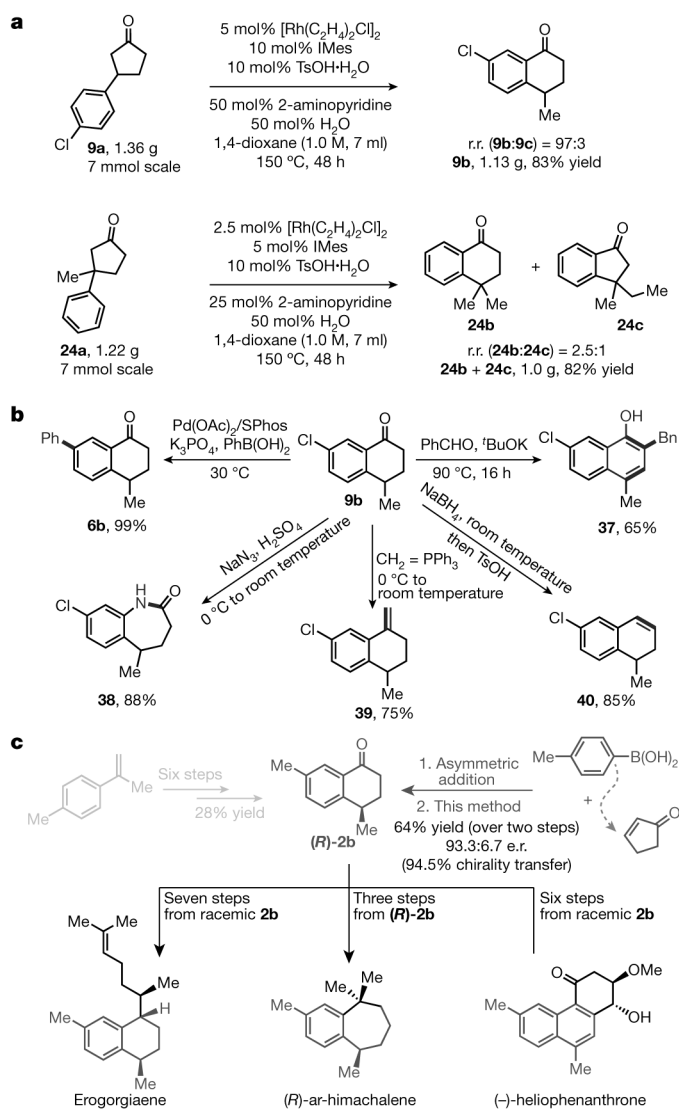


Figure 3. Gram-scale synthesis and synthetic applications

a, Gram-scale reactions. Compared with the small-scale reaction, using substrate **9a** in a gram-scale reaction produced a higher percentage yield; similarly, when using substrate **24a**, less catalyst was needed. **b**, Standard protocols can be used to add several new functional groups to our C–C activation product α -tetralone **9b**. Bn, benzyl group. **c**, Applications in asymmetric total syntheses of terpenoids. It is known that α -tetralone (**2b**) is an intermediate for accessing erogorgiaene^{20,21}, (*R*)-ar-himachalene²² and (–)-heliophenanthrone²³ in three to seven steps (shown at the bottom). However, enantioselective preparation of α -tetralones with a C4 stereocentre is non-trivial and generally requires many steps²² (top left, pale grey). In our technique (top right, dark grey), we synthesized optically enriched 3-arylcyclopentanones in a single step through asymmetric conjugate addition of cyclopentenone and arylboronic acids²⁴; then, using our C–C activation approach, we isolated α -tetralone (**(R)-2b**) in 64% yield over two steps, with 94.5% chirality transfer. e.r., enantiomeric ratio.

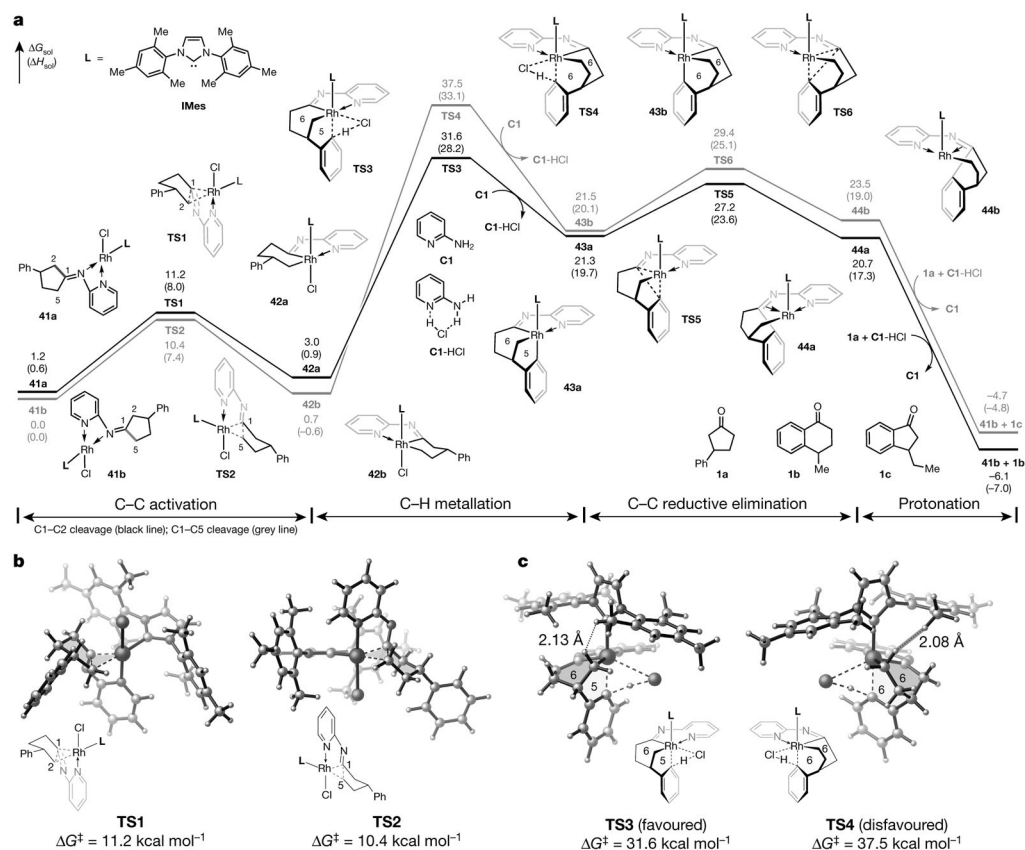


Figure 4. DFT-computed pathways for the activation of C–C bonds in cyclopentanones
a, The computed reaction energy profile of the reaction with cyclopentanone **1a**. **L**, ligand; **TS**, transition state; G_{sol}^{\ddagger} , Gibbs free energy with respect to **41b** (given in kcal mol⁻¹); H_{sol}^{\ddagger} , enthalpy with respect to **41b** (given in kcal mol⁻¹). **b**, Transition states during C–C bond activation. G^{\ddagger} , Gibbs free energy of activation. **c**, Transition states during C–H bond cleavage. Energies are computed at the M06/SDD–6-311+G(d,p)/SMD (1,4-dioxane) level of theory, with geometries optimized at the B3LYP/LANL2DZ–6-31G(d) level (see Supplementary Information for more details and references).